JPET Fast Forward. Published on May 30, 2012 as DOI: 10.1124/jpet.112.193813

Differences in Early Acetaminophen Hepatotoxicity Between Obese ob/ob and db/db Mice

Jacinthe Aubert, Karima Begriche, Matthieu Delannoy, Isabelle Morel, Julie Pajaud, Catherine Ribault, Sylvie Lepage, Mitchell R. McGill, Catherine Lucas-Clerc, Bruno Turlin, Marie-Anne Robin, Hartmut Jaeschke, and Bernard Fromenty

INSERM, U991 (J.A., K.B., M.D., I.M., J.P., C.R., M.-A.R., B.F.) and Plate-forme d'Histopathologie H2P2, Biosit (B.T.), Université de Rennes 1; Laboratoire de Toxicologie Biologique et Médico-légale (I.M., S.L.), Laboratoire de Biochimie Générale, (C.L.-C.), and Département d'Anatomie et Cytologie Pathologiques (B.T.), Hôpital Pontchaillou Rennes, France; Department of Pharmacology, Toxicology and Therapeutics, University of Kansas Medical Center (M.R.M., H.J.), Kansas City, KS, USA

JPET Fast Forward. Published on May 30, 2012 as DOI: 10.1124/jpet.112.193813
This article has not been copyedited and formatted. The final version may differ from this version.

Running title: Acetaminophen-induced liver injury in obese mice

Corresponding author :

Bernard Fromenty
INSERM**,** U991, Université de Rennes 1, 35000 Rennes, France.
E-mail: bernard.fromenty@inserm.fr
Tel.: +33 2 23 23 30 44; fax: +33 2 23 23 53 85

Statistics:

Number of text pages: 29 (all pages included)
Number of tables: 3
Number of figures: 6
Number of references: 60
Number of words in the Abstract: 250
Number of words in the Introduction: 565
Number of words in the Discussion: 940

ABBREVIATIONS: ACO, acyl-coenzyme A oxidase; ALF, acute liver failure, ALT, alanine aminotransferase; APAP, acetaminophen; AST, aspartate aminotransferase; CYP2E1, cytochrome P450 2E1; γGCS, γ-glutamylcysteine synthetase; GSH, reduced glutathione; GST, glutathione S-transferase; HO-1, heme oxygenase-1; Hsp70, heat shock proteins 70; IGFBP-1, insulin-like growth factor binding protein-1; JNK, c-jun N-terminal kinase; L-CPT1, L-carnitine palmitoyltransferase; NAFLD, nonalcoholic fatty liver disease; NAPQI, N-acetyl-*p*-benzoquinone imine; NASH, nonalcoholic steatohepatitis; Nrf2, NF-E2-related factor-2; PDK4, pyruvate dehydrogenase kinase 4; PPARα, peroxisome proliferator activated receptor-α; Trib3, Tribbles homolog 3; TUNEL, terminal deoxynucleotidyl transferase-mediated dUTP nick-end labeling.

Recommended section: Toxicology

JPET Fast Forward. Published on May 30, 2012 as DOI: 10.1124/jpet.112.193813
This article has not been copyedited and formatted. The final version may differ from this version.

ABSTRACT

Clinical investigations suggest that hepatotoxicity after acetaminophen (APAP) overdose could be more severe in the context of obesity and nonalcoholic fatty liver disease. The pre-existence of fat accumulation and cytochrome P450 2E1 (CYP2E1) induction could be major mechanisms accounting for such hepatic susceptibility. To explore this issue, experiments were performed in obese and diabetic ob/ob and db/db mice. Preliminary investigations performed in male and female wild-type, ob/ob and db/db mice showed a selective increase in hepatic CYP2E1 activity in female db/db mice. However, liver triglycerides in these animals were significantly lower compared to ob/ob mice. Next, APAP (500 mg/kg) was administered in female wild-type, ob/ob and db/db mice and investigations were carried out 0.5, 2, 4 and 8 h after APAP intoxication. Liver injury 8 h after APAP intoxication was higher in db/db mice, as assessed by plasma transaminases, liver histology and TUNEL assay. In db/db mice, however, the extent of hepatic glutathione depletion, levels of APAP-protein adducts, c-jun N-terminal kinase (JNK) activation, changes in gene expression and mitochondrial DNA levels were not greater compared to the other genotypes. Furthermore, in the db/db genotype, plasma lactate and β-hydroxybutyrate were not specifically altered, whereas plasma levels of APAP-glucuronide were intermediary between wild-type and ob/ob mice. Thus, early APAP-induced hepatotoxicity was greater in db/db than in ob/ob mice, despite less severe fatty liver and similar basal levels of transaminases. Hepatic CYP2E1 induction could have an important pathogenic role when APAP-induced liver injury occurs in the context of obesity and related metabolic disorders.

JPET Fast Forward. Published on May 30, 2012 as DOI: 10.1124/jpet.112.193813
This article has not been copyedited and formatted. The final version may differ from this version.

Introduction

Acetaminophen (N-acetyl-*p*-aminophenol, or APAP) is one of the most widely prescribed drugs for the management of pain and hyperthermia. This drug is mainly metabolized in the liver by phase II conjugating enzymes into the harmless glucuronide and sulfate conjugates, which represent in the urine about 55% and 30% of the initial APAP dose, respectively (Prescott, 1980). In addition, a small amount of APAP is oxidized to the highly reactive metabolite N-acetyl-*p*-benzoquinone imine (NAPQI) by several cytochromes P450, and more specifically by cytochrome P450 2E1 (CYP2E1) (Dahlin et al., 1984; Gonzalez, 2007). Although NAPQI is safely detoxified by hepatic reduced glutathione (GSH) when APAP is taken at the recommended dosage, high levels of NAPQI after overdose can induce several detrimental effects. Indeed, hepatocellular GSH stocks are quickly depleted and, as soon as GSH is no longer available for NAPQI detoxication, this reactive metabolite binds to different macromolecules, including proteins (Tirmenstein and Nelson, 1989; Muldrew et al., 2002). Importantly, these early cellular events are followed by c-jun N-terminal kinase (JNK) activation, mitochondrial dysfunction, overproduction of reactive oxygen species (ROS) and peroxynitrite, massive hepatocellular necrosis and acute liver failure (ALF) (Cover et al., 2005; Jaeschke and Bajt, 2006; Hinson et al., 2010).

Although APAP is usually deemed a safe drug, APAP intoxication is relatively common, in particular in the context of unintentional overdosage (Larson et al., 2005; Craig et al., 2011). Several predisposing factors could enhance the risk and the severity of APAP-induced ALF, including malnutrition, alcoholic liver disease, hepatitis C virus infection and nonalcoholic fatty liver disease (NAFLD), which is often associated with obesity and type 2 diabetes (Nguyen et al., 2008; Myers and Shaheen, 2009). NAFLD encompasses a large spectrum of liver lesions such as fatty liver, nonalcoholic steatohepatitis (NASH) and cirrhosis (Diehl, 2002; Trak-Smayra et al., 2011). Importantly, hepatic CYP2E1 activity is frequently enhanced in obese individuals with NAFLD (Chalasani et al., 2003; Aubert et al., 2011), and in type 2 diabetics (Wang et al., 2003).

Different investigations in rodents have dealt with APAP-induced hepatotoxicity in the context of obesity, type 2 diabetes and NAFLD. However, these investigations have shown conflicting results. Indeed, whereas some studies showed increased hepatotoxicity (Corcoran and Wong, 1987; Kon et al., 2010; Kučera et al., 2012), others demonstrated no difference, or an obvious protection (Blouin et al., 1987; Ito et al., 2006; Sawant et al., 2006). Although the exact reasons for this discrepancy are currently unknown, several hypotheses can be put forward. Firstly, hepatic CYP2E1 activity can significantly vary between the different rodent models of obesity (Aubert et

JPET Fast Forward. Published on May 30, 2012 as DOI: 10.1124/jpet.112.193813
This article has not been copyedited and formatted. The final version may differ from this version.

al., 2011). Secondly, obesity and NAFLD seem to be associated with increased APAP glucuronidation and clearance (Xu et al., 2012), and this could have afforded protection against APAP-induced liver injury in some studies. Thirdly, basal levels of oxidative stress and mitochondrial dysfunction, as well as lipid accumulation in liver can also greatly fluctuate between these models. The extent of lipid accretion could be a critical factor since it can sensitize cells to cell death induced by different types of insults (Feldstein et al., 2003; Reinartz et al., 2010). Thus, the main goal of the present study was to obtain information concerning the factors that could significantly modulate APAP-induced hepatotoxicity in the context of obesity and related metabolic disorders. To this end, we performed investigations in obese (ob/ob) and diabetic (db/db) mice presenting fatty liver with or without high hepatic CYP2E1 activity, respectively.

JPET Fast Forward. Published on May 30, 2012 as DOI: 10.1124/jpet.112.193813
This article has not been copyedited and formatted. The final version may differ from this version.

Materials and Methods

Animals. All mice were purchased from Janvier (Le-Genest-St-Isle, France). After their arrival at the animal facility, mice were acclimatized for at least 1 week in an environmentally controlled room with 12 h light/dark cycle and free access to food and water. In this study, wild-type C57BL/6J-+/+ (henceforth referred to as wild-type mice), C57BL/6J-ob/ob mice (ob/ob mice) and C57BL/KsJ-db/db mice (db/db mice) were used for all investigations. Importantly, a recent study showed that wild-type C57BL/6J and C57BL/KsJ mice were similarly susceptible to APAP-induced liver injury (Harrill et al., 2009). In a first series of preliminary investigations, 10-week-old male and female wild-type, ob/ob and db/db mice were used in order to determine hepatic CYP2E1 activity. Thereafter, 10- to 12-week-old female wild-type, ob/ob and db/db mice were used for all experiments dealing with APAP-induced hepatotoxicity. In these experiments, mice were treated with APAP (Sigma-Aldrich, St. Quentin-Fallavier, France) or the vehicle control after an overnight fast. To this end, APAP was dissolved in warm saline and injected intraperitoneally at the dose of 500 mg/kg body weight, whereas saline was administered to control animals. After 0.5, 2, 4 or 8 h, blood was drawn from the retro orbital sinus with heparinized capillary Pasteur pipettes for biochemistry analyses. Mice were then sacrificed by cervical dislocation and liver was quickly removed. While a majority of the liver fragments were immediately frozen in liquid nitrogen, some of them were rapidly processed for appropriate histological staining. Collected liver fragments frozen in liquid nitrogen were subsequently stored at -80°C until use. All experiments were performed according to national guidelines for the use of animals in biomedical research and approved by the local Ethics Committee in Animal Experiment of Rennes 1 University.

Plasma Studies. Immediately after collection, blood was centrifuged for 10 min at 1000*g* and plasma was stored at -20°C until assay. Plasma activity of alanine aminotransferase (ALT) and aspartate aminotransferase (AST) and glucose levels were measured on an automatic analyser AU2700 (Olympus Diagnostics, Rungis, France) with Olympus commercial Kits OSR6107, OSR6109 and OSR6121, respectively. Plasma lactate and β-hydroxybutyrate were measured with commercial kits purchased from Biovision Inc. (Mountain View, CA) and Cayman Chemical Company (Ann Arbor, MI), respectively. Plasma levels of APAP, APAP-glucuronide and APAP-sulfate were measured using an LC-MS/MS system from Thermo Scientific (San Jose, CA). Briefly, separation of the analytes was carried out on a Thermo Hypersil Gold C18 column (3.0 µm, 2.1 x 100 mm). The mobile phase consisted of aqueous 1% formic acid and 95% methanol (80:20, v/v). Calibration or mouse plasma (25 µl) samples were supplemented with deuterated APAP (Promochem, Molsheim, France) as internal standard, and treated with methanol. The retention

JPET Fast Forward. Published on May 30, 2012 as DOI: 10.1124/jpet.112.193813
This article has not been copyedited and formatted. The final version may differ from this version.

times for APAP-glucuronide, APAP-sulfate, APAP and internal standard were 2.3, 2.9, 3.5 and 3.5 min, respectively. Data acquisition, peak integration and calibration were performed using Xcalibur® 2.1 software.

Liver Histology and Terminal Deoxynucleotidyl Transferase-Mediated dUTP Nick-End Labeling (TUNEL) Assay. To evaluate the different hepatic lesions, liver fragments were fixed in 10% neutral formalin and embedded in paraffin. Then, 4-µm thick sections were cut, stained with hematoxylin, eosin and safran (HES), and blindly examined by an experienced pathologist (BT). After the examination of 10 different liver lobules per mouse, a score of necrosis from 0 to 3 was given based on the surface of the necrotic areas and the nature of the cytoplasmic and nuclear alterations. HES staining was also used in order to evaluate the presence of macrovacuolar and microvesicular steatosis. Cell death was assessed with the TUNEL assay using the In Situ Cell Death Detection Kit purchased from Roche Diagnostics (Indianapolis, IN), according to the manufacturer's recommendations.

Reduced GSH and APAP-Protein Adducts in Liver. Reduced GSH was determined by an enzymatic reaction in which it reduces 5, 5'-dithio-bis(2-nitrobenzoic acid) to generate 2-nitro-5-thiobenzoic acid that is spectrophotometrically measured at 412 nm (Robin et al., 2005a). For the assessment of APAP-protein adducts, APAP-cysteine (APAP-CYS) was measured using high-pressure liquid chromatography separation and electrochemical detection, as previously described (Muldrew et al., 2002).

CYP2E1 and Caspase 3 Activities. CYP2E1 activity was assessed on hepatic microsomes, as previously described (Robin et al., 2005b). To prepare microsomes, liver fragments (ca. 500 mg) were homogenized in 5 ml of 50 mM Tris buffer supplemented with sucrose 0.25 M, EDTA 1 mM, PMSF 25 µM and DTT 1mM (pH 7.4), and the homogenate was centrifuged at 1,000*g* for 10 min at 4°C. The supernatant (liver tissue homogenate) was subsequently centrifuged at 9,000*g* for 20 min at 4°C. The new supernatant was finally centrifuged at 100,000*g* for 1 h at 4°C. The pellet (microsomal fraction) was resuspended in 200 µl of 0.1 M sodium phosphate buffer (pH 7.4) containing 10% glycerol, and was stored at -80 °C until use. Microsomal proteins were determined by the method of Lowry, based on the Folin phenol reagent. CYP2E1 activity was subsequently assessed by measuring hydroxylation of aniline into *p*-aminophenol (Robin et al., 2005b) and hydroxylation of chlorzoxazone into 6-hydroxychlorzoxazone (Guillouzo and Chesne, 1996). Hepatic caspase 3 activity was assessed in liver homogenates, as previously described (Dumont et al., 2010).

Western Blot Analysis. To assess liver expression of total and phosphorylated JNK1/2 (JNK1/2 and phospho-JNK1/2, respectively), hepatic proteins underwent SDS-polyacrylamide electrophoresis. Briefly, liver fragments were homogenized in a lysis buffer (Cell Signaling

JPET Fast Forward. Published on May 30, 2012 as DOI: 10.1124/jpet.112.193813
This article has not been copyedited and formatted. The final version may differ from this version.

Technology Inc., Danvers, MA) supplemented with 1mM PMSF. Homogenates were then centrifuged at 4,500*g* at 4 °C to remove tissue debris. Forty µg of protein were then separated by electrophoresis on 4-12% gradient Bis-Tris gels (Invitrogen, Cergy-Pontoise, France), transferred to Hybond ECL nitrocellulose membranes (Amersham Biosciences, Little Chalfont, UK) and immunoblotted with antibodies against JNK1/2 (Santa Cruz Biotechnology, Santa Cruz, CA), phospho-JNK1/2 (Thr183/Tyr185) (Calbiochem, San Diego, CA), and Hsc70 (Tebu-bio, Le Perray en Yvelines, France). Blots were then incubated with appropriate secondary antibodies, and protein bands were revealed by enhanced chemiluminescence in a Chemi-smart imager (Fisher Scientific, Illkirch, France). Heat shock cognate protein 70 (Hsc70) was used to normalize protein loadings, and quantification was performed with the BIO-1D software. In order to correlate JNK phosphorylation status to its activity, the nonradioactive SAPK/JNK Kinase Assay kit (Cell Signaling Technology Inc.) was used, according to the manufacturer's recommendations.

Real-Time Quantitative PCR (RT-qPCR) Analysis. In order to study gene expression in liver, total RNA was extracted with the SV Total RNA Isolation System from Promega (Madison, WI), which included a direct DNase treatment step. RNA quantity and purity were assessed with a Nanodrop ND-1000 spectrophotometer (Nyxor Biotech, Paris, France), whereas RNA integrity was checked after migration on a 1% agarose gel. cDNAs were prepared by reverse transcription of 1 µg of total RNA using the High Capacity cDNA Reverse Transcription Kit (Applied Biosystems, Courtaboeuf, France). cDNAs were thus amplified with specific primers using the Power SYBR Green PCR Master Mix (Applied Biosystems), in an ABI Prism 7900 instrument (Applied Biosystems). The PCR conditions were one cycle at 50°C for 2 min and one cycle at 95°C for 10 min followed by 40 cycles at 95°C for 15 s and 60°C for 1 min. Amplification of specific transcripts was confirmed by melting curve profiles generated at the end of each run. Moreover, PCR specificity was further ascertained with a 1.75% agarose gel electrophoresis by checking the length of the PCR products. Expression of the mouse ribosomal protein S6 (S6) was used as reference, and the $2^{-\Delta\Delta Ct}$ method was used to express the relative expression of each selected gene (Begriche et al., 2008a; Massart et al., 2012). Quantification of the mitochondrial DNA (mtDNA) was also performed by RT-qPCR after extraction of total genomic DNA using the Qiagen DNeasy tissue kit (Qiagen, Courtaboeuf, France). Briefly, 20 mg liver samples were digested in a lysis buffer supplemented with proteinase K. After complete tissue digestion, genomic DNA was then extracted and purified according to the manufacturer recommendations. mtDNA levels were then assessed by RT-qPCR using primers specific to the mitochondrial cytochrome *c* oxidase II (COX II) gene, whereas the nuclear DNA-encoded S6 gene was used for normalization. Sequences of the primers used in this study are available on request.

JPET Fast Forward. Published on May 30, 2012 as DOI: 10.1124/jpet.112.193813
This article has not been copyedited and formatted. The final version may differ from this version.

Statistical Analyses. Data are presented as means ± SEM (standard error of mean). Analysis of variance (ANOVA) was performed in order to assess statistical significances. For the preliminary investigations carried out with male and female wild-type, ob/ob and db/db mice, a two-way ANOVA was used with the factors of sex and genotype. For the subsequent experiments performed with female wild-type, ob/ob and db/db mice treated with APAP or vehicle control, a two-way ANOVA was performed with the factors of genotype and APAP treatment. The one-way ANOVA and Mann and Whitney tests were used in some experiments. When ANOVA provided significant differences, individual means were compared with the Tukey's HSD (Honestly Significant Difference) test.

JPET Fast Forward. Published on May 30, 2012 as DOI: 10.1124/jpet.112.193813
This article has not been copyedited and formatted. The final version may differ from this version.

Results

Preliminary Investigations in Lean and Obese Mice. The present study was performed to obtain information concerning factors that could significantly modulate APAP-induced hepatotoxicity in the context of obesity and NAFLD. In particular, we wished to determine whether hepatic CYP2E1 induction and/or the degree of fatty liver could have a significant effect on early APAP-induced liver injury.

CYP2E1 plays a key role in APAP hepatotoxicity, as this enzyme generates the toxic metabolite NAPQI (Jaeschke and Bajt, 2006; Gonzalez, 2007). Moreover, hepatic CYP2E1 activity is frequently enhanced in obese individuals with associated metabolic diseases such as NAFLD and type 2 diabetes (Chalasani et al., 2003; Aubert et al., 2011). However, to the best of our knowledge, hepatic CYP2E1 activities in male and female wild-type, ob/ob and db/db mice have never been compared in the same study. In a first set of preliminary investigations, we found that microsomal CYP2E1-mediated aniline and chlorzoxazone hydroxylase activities were significantly increased in female db/db mice compared to the other groups of animals (Table 1). Moreover, there was a positive correlation between plasma glucose (Table 1) and CYP2E1-mediated aniline hydroxylase activity in liver (r^2=0.315, $p<0.01$), supporting previous data about a possible role of type 2 diabetes in hepatic CYP2E1 induction (Aubert et al., 2011). Thus, female db/db mice were selected in the present study as a murine model of obesity associated with hepatic CYP2E1 induction. Importantly, several investigations in mice of different genetic background (including C57BL/6) showed that APAP biotransformation and toxicity significantly varied between males and females (Dai et al., 2006; Lee et al., 2009; Masubuchi et al., 2011). Hence, only females of the different mouse genotypes were selected for further investigations.

The degree of fatty liver is another factor which could play a significant role in APAP-induced liver injury in the context of obesity. Indeed, excess lipid can sensitize cells to cell death induced by different types of insults (Feldstein et al., 2003; Reinartz et al., 2010). In this study, hepatic fat deposition was higher in female ob/ob mice with a combination of macrovacuolar and microvesicular steatosis, whereas steatosis was mostly microvesicular in female db/db mice (Figure 1A). Moreover, liver triglycerides were significantly enhanced by 134% in female ob/ob mice compared with female db/db mice (Figure 1B). These data are in keeping with previous results also obtained in female ob/ob and db/db mice (Sahai et al., 2004). Greater lipid deposition in ob/ob mice also explained higher liver weight and liver to body weight ratio in these animals (Table 1). Finally, liver lipids in female wild-type mice (n=6) were much lower compared to the obese animals as total lipids and triglycerides were 18 ± 3 and 4 ± 1 $mg.g^{-1}$ liver, respectively.

JPET Fast Forward. Published on May 30, 2012 as DOI: 10.1124/jpet.112.193813
This article has not been copyedited and formatted. The final version may differ from this version.

Early Hepatotoxicity after APAP Intoxication in Female Wild-Type, ob/ob and db/db Mice. In order to evaluate APAP-induced liver injury, 500 mg/kg of APAP was administered to female wild-type, ob/ob and db/db mice and plasma transaminases were determined 0.5, 2, 4 and 8 h after APAP intoxication. Importantly, basal activity of transaminases was higher in obese mice (Figure 2A), reflecting the presence of moderate hepatic cytolysis associated to NASH. Whereas plasma transaminases were unchanged in all groups of mice 0.5 h after APAP administration (data not shown), activity of transaminases was significantly enhanced after 2 h, but only in wild-type mice (609 ± 144 and 2542 ± 614 UI/L, respectively for ALT and AST; n=6-7 mice). After 4 h, plasma transaminases were significantly enhanced in all groups of treated mice, although there was no difference between the different genotypes. Indeed, ALT activity was 1022 ± 328, 783 ± 176 and 619 ± 136 UI/L, whereas AST values were 1495 ± 412, 1603 ± 368 and 1291 ± 239 UI/L, respectively in wild-type, ob/ob and db/db mice (n=9-12 animals per group).

After 8 h, plasma transaminases were further enhanced in the different groups of treated mice, but particularly in db/db mice (Figure 2B). Indeed, AST and ALT activity in db/db mice was increased by 2- or 3-fold compared to wild-type and ob/ob mice. In all mice, the areas of cytolysis were generally located around the central veins (i.e. where CYP2E1 is mainly expressed), although in some obese mice these areas extended to the mediolobular zones (Figure 2C). When a score of necrosis was attributed as described in the Methods, all treated wild-type (n=9) mice were scored 2, whereas 1, 6 and 2 ob/ob mice were scored 0, 1 and 3, respectively. For the db/db genotype, 1, 5 and 3 mice were scored 1, 2 and 3, respectively. Thus, necrosis was in general less severe in ob/ob mice whereas the highest frequency of score 3 was observed in db/db mice. Interestingly, APAP intoxication in wild-type mice induced macrovacuolar steatosis in some hepatocytes (Figure 2C), as previously described in humans and mice (Yohe et al., 2006; Begriche et al., 2011). Moreover, APAP intoxication aggravated steatosis in obese mice, in particular in ob/ob mice (Figure 2C). Finally, a TUNEL assay was performed and the percentage of TUNEL-positive nuclei was measured in the different groups of mice. As shown in Figure 3, the TUNEL-positive nuclei were located around the central vein, and the percentage of these nuclei was significantly higher in db/db mice compared to ob/ob mice. However, measurement of caspase 3 activity showed virtually no activity of this enzyme, whatever the group of treated mice (data not shown). This result is in keeping with previous investigations showing that hepatic necrosis, rather than apoptosis, is the major pathway of cell death after APAP intoxication (Jaeschke and Bajt, 2006; Han et al., 2010; Hinson et al., 2010).

GSH and APAP-Protein Adducts in Liver. Early APAP hepatotoxicity is associated with a rapid depletion of liver GSH reserves, as well as covalent binding of NAPQI to macromolecules, including proteins (Tirmenstein and Nelson, 1989; Muldrew et al., 2002; Jaeschke and Bajt, 2006).

JPET Fast Forward. Published on May 30, 2012 as DOI: 10.1124/jpet.112.193813
This article has not been copyedited and formatted. The final version may differ from this version.

In this study, decreased GSH and increased APAP-protein adducts in liver were observed 0.5, 2, 4 and 8 h after APAP intoxication in all groups of mice, although there were some differences between wild-type and obese mice (Figure 4). Indeed, GSH depletion and recovery occurred earlier in wild-type mice compared with ob/ob and db/db mice (Figure 4A). Levels of APAP-protein adducts in liver reached a plateau as soon as 2 h in wild-type mice, but only after 4 h in ob/ob and db/db mice. In addition, levels of APAP-protein adducts in obese mice after 0.5, 2 and 8 h were significantly lower compared to wild-type mice (Figure 4B).

Total and Phosphorylated JNK in Liver. APAP hepatotoxicity is associated with a rapid phosphorylation of JNK, inducing its activation which then enhances mitochondrial dysfunction and other detrimental cellular events (Han et al., 2010; Hinson et al., 2010). In this study, JNK phosphorylation was observed 2, 4 and 8 h after APAP intoxication (Figure 5), but not after 0.5 h (data not shown). After 2 h, JNK was phosphorylated in all wild-type mice, but only in a few obese mice (1 out of 3 animals in each genotype). After 4 h, JNK was phosphorylated in all mice, but there was no significant difference between genotypes. After 8 h, JNK phosphorylation was still high in ob/ob mice, but was reduced in wild-type and db/db mice (Figure 5). Measurement of hepatic JNK activity was in keeping with these results, with a trend towards lower JNK activation in ob/ob and db/db mice after 2 h, and higher JNK activity in ob/ob mice after 8 h (data not shown).

Hepatic mRNA Expression of Genes After APAP Intoxication. After APAP intoxication, there is a rapid alteration in the hepatic expression of numerous genes involved in oxidative stress and antioxidant defence, glutathione synthesis, APAP metabolism, cell repair and lipid homeostasis, including mitochondrial and peroxisomal fatty acid oxidation (Heinloth et al., 2004; Beyer et al., 2007). In this study, hepatic expression of the following genes were determined after APAP administration: NF-E2-related factor-2 (Nrf2), heme oxygenase-1 (HO-1), heat shock proteins 70 (Hsp70), insulin-like growth factor binding protein-1 (IGFBP-1), γ-glutamylcysteine synthetase (γGCS), Tribbles homolog 3 (Trib3), glutathione S-transferases pi-1 and kappa (GSTP1 and GSTK), peroxisome proliferator activated receptor-α (PPARα), L-carnitine palmitoyltransferase (L-CPT1), acyl-coenzyme A oxidase (ACO), pyruvate dehydrogenase kinase 4 (PDK4). Recent investigations showed that increased Trib3 expression was a good marker to detect GSH depletion secondary to its conjugation (Gao et al., 2010), and that high basal PDK4 expression could increase sensitivity to APAP-induced hepatotoxicity (Liu et al., 2010). As shown in Figure 6A, the expression of several of these genes was up-regulated as early as 0.5 h after APAP administration, especially IGFBP-1, γGCS, Trib3 and PDK4. Expression of these four genes was still increased after 2, 4 and 8 h (Figure 6B-D). Interestingly, γGCS expression was particularly enhanced in wild-type mice 0.5 and 2 h after APAP intoxication (Figure 6A-B), whereas γGCS up-regulation was

JPET Fast Forward. Published on May 30, 2012 as DOI: 10.1124/jpet.112.193813
This article has not been copyedited and formatted. The final version may differ from this version.

principally observed in obese mice after 8 h (Figure 6D). Since γGCS is a key enzyme of the GSH biosynthetic pathway, these results could explain, at least in part, why recovery of liver GSH was faster in wild-type mice compared to ob/ob and db/db mice (Figure 4A). HO-1 expression was highly up-regulated 2 h after APAP intoxication in wild-type mice and afterward in all genotypes (Figure 6B-D). A reduction of PPARα expression was observed 2, 4 and 8 h after APAP administration. Interestingly, 8 h after APAP administration, expression of PPARα and of its targets L-CPT1 and ACO was particularly decreased in obese mice (Figure 6D). Moreover, at this time point, expression of the mitochondrial fatty acid oxidation enzyme medium-chain acyl-CoA dehydrogenase (another PPARα target) was significantly reduced in ob/ob and db/db mice by 32 and 37%, respectively, whereas it was unchanged in wild-type mice (data not shown). Significant reduction of the PPARα signaling pathway in ob/ob and db/db mice could be one mechanism explaining the aggravation of fatty liver in these obese animals (Figure 2).

Hepatic mtDNA Levels. APAP intoxication in mice can induce early mtDNA depletion in liver (Cover et al., 2005). In the present study, hepatic mtDNA levels were significantly decreased by 32% in ob/ob mice 2 h after APAP intoxication, but mtDNA depletion was not observed in the other groups of treated mice (Table 2). In addition, whereas mtDNA was virtually unchanged 4 h after APAP treatment in all groups of animals, mtDNA levels were significantly enhanced after 8 h in all treated mice (Table 2). It was also noteworthy that basal hepatic mtDNA levels were increased in ob/ob mice, as previously reported (Robin et al., 2005a). Increased mtDNA levels in liver could be an adaptive response to oxidative stress (Robin et al., 2005a).

Plasma Lactate and β-Hydroxybutyrate. Drug-induced mitochondrial dysfunction can induce hyperlactatemia (or lactic acidosis) and complex changes in plasma ketone bodies acetoacetate and β-hydroxybutyrate (Fromenty and Pessayre, 1995; Labbe et al., 2008). Indeed, although plasma ketone bodies are classically reduced when hepatic fatty acid oxidation is impaired, plasma levels of these oxidative products can be paradoxically enhanced when Krebs cycle is inhibited in extra-hepatic tissues (Fromenty and Pessayre, 1995; Labbe et al., 2008). In this study, plasma lactate was decreased in mice 2, 4 and 8 h after APAP administration, in particular in ob/ob mice (Table 2). Interestingly, plasma glucose in ob/ob mice was significantly reduced by 47 and 57%, respectively 4 and 8 h after APAP administration (data not shown). Thus, reduced glucose availability might have reduced lactate production in ob/ob mice. Plasma β-hydroxybutyrate levels were significantly decreased 4 h after APAP administration in all genotypes, but especially in obese mice (Table 2). After 2 and 8 h, however, plasma β-hydroxybutyrate was either decreased, or increased, in the different groups of animals (Table 2).

JPET Fast Forward. Published on May 30, 2012 as DOI: 10.1124/jpet.112.193813
This article has not been copyedited and formatted. The final version may differ from this version.

Plasma levels of APAP, APAP-sulfate and APAP-glucuronide. Finally, plasma levels of APAP, APAP-sulfate and APAP-glucuronide were determined in treated mice 0.5, 2, 4 and 8 hr after APAP intoxication (Table 3). After 0.5 and 2 h, APAP levels were higher in obese mice compared to wild-type, whereas the converse was observed later on. Levels of APAP-sulfate were significantly higher in ob/ob and db/db obese mice compared to wild-type mice, but only 2 h after APAP administration. Lastly, APAP-glucuronide levels after 0.5 and 2 h were significantly increased in obese mice compared to wild-type mice (Table 3). Interestingly, whatever the time points, levels of APAP-glucuronide were always the highest in ob/ob mice. This is in keeping with recent investigations showing higher APAP glucuronidation in hepatic microsomes from ob/ob mice compared to wild-type mice (Xu et al., 2012).

JPET Fast Forward. Published on May 30, 2012 as DOI: 10.1124/jpet.112.193813
This article has not been copyedited and formatted. The final version may differ from this version.

Discussion

The present study was carried out in order to explore the underlying mechanisms that could potentially explain why NAFLD enhances the severity of APAP-induced hepatotoxicity. Our data clearly indicated that the degree of fatty liver in obese mice was not a key pathogenic factor in early hepatotoxicity induced by 500 mg/kg APAP. Indeed, whereas basal levels of hepatic triglycerides was lower in db/db mice compared to ob/ob mice, liver injury 8 h after APAP intoxication was significantly higher in the former group. Moreover, APAP-induced hepatic cytolysis was about similar between wild-type and ob/ob mice.

Leptin-deficient ob/ob mice and leptin-resistant db/db mice are widely used as models of obesity, type 2 diabetes and NAFLD. One of the major advantages of these genetic murine models of obesity is the rapid and consistent occurrence of insulin resistance, hyperglycemia and NAFLD (Lindström, 2007; Trak-Smayra et al., 2011; Massart et al., 2012), whereas high-fat diet-induced obesity is not always associated with these secondary metabolic disorders, even after several months of feeding (Burcelin et al., 2002; Begriche et al., 2008a). It is noteworthy that both ob/ob and db/db mice are characterized by "borderline NASH", as fatty liver is associated with moderate hepatic necroinflammation and mild fibrosis (Li et al., 2003; Begriche et al., 2008b; Trak-Smayra et al., 2011). Moreover, this study and previous investigations (Trak-Smayra et al., 2011) showed comparable basal levels of plasma transaminases between ob/ob and db/db mice, thus indicating a similar degree of hepatic cytolysis. However, db/db mice have less lipid deposition in liver compared to ob/ob mice (Sahai et al., 2004; Trak-Smayra et al., 2011), a feature that has been confirmed in this study.

Several experimental and clinical investigations reported that NAFLD could sensitise to drug-induced acute liver injury (Tarantino et al., 2007; Begriche et al., 2011). However, the present study indicates that fatty liver *per se* and pre-existent hepatic cytolysis are not systematically involved in this sensitisation. This strongly suggests the presence of other pathogenic factors. Although further investigations will be required to determine the exact cause(s) of higher sensitivity of db/db mice to APAP hepatotoxicity, increased basal hepatic CYP2E1 activity could have played a role. Enhanced hepatic CYP2E1 activity has been associated with more severe APAP-induced hepatotoxicity in the context of chronic ethanol intoxication (Zhao and Slattery, 2002; Gonzalez, 2007). This major role of CYP2E1 is due to the generation of NAPQI, a highly reactive metabolite that depletes GSH (Jaeschke and Bajt, 2006) and binds to different cellular proteins (Tirmenstein and Nelson, 1989; Muldrew et al., 2002).

JPET Fast Forward. Published on May 30, 2012 as DOI: 10.1124/jpet.112.193813
This article has not been copyedited and formatted. The final version may differ from this version.

In our investigations, however, depletion of GSH and levels of APAP-protein adducts in liver were not higher in db/db mice. Regarding these adducts, it is conceivable that a small subset of critical proteins could have been specifically damaged by NAPQI in db/db mice. Importantly, NAPQI could bind to, and thus inhibit, different enzymes of the plasma membrane, cytosol and mitochondria (Tsokos-Kuhn et al., 1988; Landin et al., 1996; Gupta et al., 1997). However, it is still uncertain whether APAP-induced hepatotoxicity is primarily due to APAP binding to these enzymes, or to other yet unidentified critical proteins. Moreover, the cellular targets of NAPQI could be different in female db/db mice. Nevertheless, our data strongly suggested that subtle events down-stream APAP metabolic activation were responsible for the higher susceptibility of db/db mice. In this respect, it is noteworthy that recent investigations in IL-4$^{-/-}$ mice showed higher susceptibility to APAP-induced liver injury despite lower levels of APAP-protein adducts (Ryan et al., 2012).

JNK activation and mitochondrial dysfunction play a significant role in APAP liver injury (Shinohara et al., 2010; Han et al., 2010; McGill et al., 2011). However, our investigations did not reveal greater hepatic JNK activation in db/db mice after APAP intoxication. Early hepatic mtDNA depletion was detected in ob/ob mice 2 h after APAP intoxication, but this was not observed in db/db mice. Later on, 8 h after APAP administration, mtDNA levels were increased in treated mice whatever the genotype. Plasma levels of lactate and β-hydroxybutyrate were also measured as surrogate markers of mitochondrial dysfunction (Fromenty and Pessayre, 1995; Labbe et al., 2008). However, after APAP treatment, plasma concentrations of lactate were decreased in all groups of mice, especially in ob/ob mice. In addition, plasma levels of β-hydroxybutyrate were either increased or decreased in db/db mice, but the extent of these changes were also greater in ob/ob mice. Lastly, hepatic expression of the mitochondrial enzymes CPT-1, PDK4 and GSTK was similarly modified after APAP treatment in the different groups of animals. Further investigations will be needed in order to determine whether specific mitochondrial alterations could have been responsible for increased APAP hepatotoxicity in db/db mice.

Obesity is a major issue for health as it is associated with several metabolic disorders including insulin resistance, type 2 diabetes and NAFLD. Moreover, there is increasing evidence that obesity and NAFLD can increase the risk and the severity of liver injury induced by several drugs. Indeed, in addition to APAP, this is suspected for halothane, tamoxifen, irinotecan, methotrexate and some antibiotics (Tarantino et al., 2007; Aubert et al., 2011; Begriche et al., 2011). Obesity and NAFLD also favor hepatotoxicity of toxic compounds such as ethanol, carbon tetrachloride and thioacetamide (Robin et al., 2005a; Donthamsetty et al., 2007; Kučera et al., 2011). Interestingly, CYP2E1 metabolizes several of these drugs and toxic derivatives, and hepatic CYP2E1 activity is frequently enhanced in obese individuals with NAFLD (Chalasani et al., 2003; Aubert et al., 2011).

Thus, along with different rodent models of diet-induced obesity and NAFLD (Aubert et al., 2011), we believe that female db/db mice could be a useful murine model in order to explore liver injury induced by these compounds.

JPET Fast Forward. Published on May 30, 2012 as DOI: 10.1124/jpet.112.193813
This article has not been copyedited and formatted. The final version may differ from this version.

Acknowledgments

We are grateful to Alain Fautrel and Pascale Bellaud from the Histopathology plate-form for their excellent technical support.

Authorship Contributions

Participated in research design: Aubert, Robin, and Fromenty.
Conducted experiments: Aubert, Begriche, Delannoy, Pajaud, Ribault, Lepage, McGill, and Lucas-Clerc.
Performed data analysis: Aubert, Morel, Turlin, Robin, and Fromenty.
Wrote or contributed to the writing of the manuscript: Aubert, Robin, Jaeschke, and Fromenty.

JPET Fast Forward. Published on May 30, 2012 as DOI: 10.1124/jpet.112.193813
This article has not been copyedited and formatted. The final version may differ from this version.

References

Aubert J, Begriche K, Knockaert L, Robin MA, and Fromenty B (2011) Increased expression of cytochrome P450 2E1 in nonalcoholic fatty liver disease: mechanisms and pathophysiological role. *Clin Res Hepatol Gastroenterol* **35**:630-637.

Begriche K, Lettéron P, Abbey-Toby A, Vadrot N, Robin MA, Bado A, Pessayre D, and Fromenty B (2008a) Partial leptin deficiency favors diet-induced obesity and related metabolic disorders in mice. *Am J Physiol Endocrinol Metab* **294**:E939-E951.

Begriche K, Massart J, Abbey-Toby A, Igoudjil A, Lettéron P, and Fromenty B (2008b) β-Aminoisobutyric acid prevents diet-induced obesity in mice with partial leptin deficiency. *Obesity* **16**:2053-2067.

Begriche K, Massart J, Robin MA, Borgne-Sanchez A, and Fromenty B (2011) Drug-induced toxicity on mitochondria and lipid metabolism: mechanistic diversity and deleterious consequences for the liver. *J Hepatol* **54**:773-794.

Beyer RP, Fry RC, Lasarev MR, McConnachie LA, Meira LB, Palmer VS, Powell CL, Ross PK, Bammler TK, Bradford BU, Cranson AB, Cunningham ML, Fannin RD, Higgins GM, Hurban P, Kayton RJ, Kerr KF, Kosyk O, Lobenhofer EK, Sieber SO, Vliet PA, Weis BK, Wolfinger R, Woods CG, Freedman JH, Linney E, Kaufmann WK, Kavanagh TJ, Paules RS, Rusyn I, Samson LD, Spencer PS, Suk W, Tennant RJ and Zarbl H (2007) Multicenter study of acetaminophen hepatotoxicity reveals the importance of biological endpoints in genomic analyses. *Toxicol Sci* **99**:326-337.

Blouin RA, Dickson P, McNamara PJ, Cibull M, and McClain C (1987) Phenobarbital induction and acetaminophen hepatotoxicity: resistance in the obese Zucker rodent. *J Pharmacol Exp Ther* **243**:565-570.

Burcelin R, Crivelli V, Dacosta A, Roy-Tirelli A, and Thorens B (2002) Heterogeneous metabolic adaptation of C57BL/6J mice to high-fat diet. *Am J Physiol Endocrinol Metab* **282**:E834-E842.

Chalasani N, Gorski JC, Asghar MS, Asghar A, Foresman B, Hall SD, and Crabb DW (2003) Hepatic cytochrome P450 2E1 activity in nondiabetic patients with nonalcoholic steatohepatitis. *Hepatology* **37**:544-550.

Corcoran GB and Wong BK (1987) Obesity as a risk factor in drug-induced organ injury: increased liver and kidney damage by acetaminophen in the obese overfed rat. *J Pharmacol Exp Ther* **241**:921-927.

Cover C, Mansouri A, Knight TR, Bajt ML, Lemasters JJ, Pessayre D, and Jaeschke H (2005) Peroxynitrite-induced mitochondrial and endonuclease-mediated nuclear DNA damage in acetaminophen hepatotoxicity. *J Pharmacol Exp Ther* **315**:879-887.

Craig DG, Bates CM, Davidson JS, Martin KG, Hayes PC, and Simpson KJ (2011) Overdose pattern and outcome in paracetamol-induced acute severe hepatotoxicity. *Br J Clin Pharmacol* **71**:273-282.

Dahlin DC, Miwa GT, Lu AY, and Nelson SD (1984) N-acetyl-p-benzoquinone imine: a cytochrome P450-mediated oxidation product of acetaminophen. *Proc Natl Acad Sci USA* **81**:1327-1331.

Dai G, He L, Chou N, and Wan YJ (2006) Acetaminophen metabolism does not contribute to gender difference in its hepatotoxicity in mouse. *Toxicol Sci* **92**:33-41.

Diehl AM (2002) Nonalcoholic steatosis and steatohepatitis IV. Nonalcoholic fatty liver disease abnormalities in macrophage function and cytokines. *Am J Physiol Gastrointest Liver Physiol* **282**:G1-G5.

Donthamsetty S, Bhave VS, Mitra MS, Latendresse JR, and Mehendale HM (2007) Nonalcoholic fatty liver sensitizes rats to carbon tetrachloride hepatotoxicity. *Hepatology* **45**:391-403.

Dumont J, Jossé R, Lambert C, Anthérieu S, Le Hegarat L, Aninat C, Robin MA, Guguen-Guillouzo C, and Guillouzo A (2010) Differential toxicity of heterocyclic aromatic amines and their mixture in metabolically competent HepaRG cells. *Toxicol Appl Pharmacol* **245**:256-263.

Feldstein AE, Canbay A, Guicciardi ME, Higuchi H, Bronk SF, and Gores GJ (2003) Diet associated hepatic steatosis sensitizes to Fas mediated liver injury in mice. *J Hepatol* **39**:978-983.

Fromenty B and Pessayre D (1995) Inhibition of mitochondrial beta-oxidation as a mechanism of hepatotoxicity. *Pharmacol Ther* **67**:101-154.

Gao W, Mizukawa Y, Nakatsu N, Minowa Y, Yamada H, Ohno Y, and Urushidani T (2010) Mechanism-based biomarker gene sets for glutathione depletion-related hepatotoxicity in rats. *Toxicol Appl Pharmacol* **247**:211-221.

Gonzalez FJ (2007) The 2006 Bernard B. Brodie Award Lecture. Cyp2e1. *Drug Metab Dispos* **35**:1-8.

Guillouzo A and Chesne C (1996) Xenobiotic metabolism in epithelial cell culture, in *Epithelial Cell Culture, A Practical Approach* (Shaw AJ ed.) pp 67-85, Oxford University press, London.

Gupta S, Rogers LK, Taylor SK, and Smith CV (1997) Inhibition of carbamyl phosphate synthetase-I and glutamine synthetase by hepatotoxic doses of acetaminophen in mice. *Toxicol Appl Pharmacol* **146**:317-327.

Han D, Shinohara M, Ybanez MD, Saberi B, and Kaplowitz N (2010) Signal transduction pathways involved in drug-induced liver injury. *Handb Exp Pharmacol* **196**:267-310.

Harrill AH, Watkins PB, Su S, Ross PK, Harbourt DE, Stylianou IM, Boorman GA, Russo MW, Sackler RS, Harris SC, Smith PC, Tennant R, Bogue M, Paigen K, Harris C, Contractor T, Wiltshire T, Rusyn I, and Threadgill DW (2009) Mouse population-guided resequencing reveals

that variants in CD44 contribute to acetaminophen-induced liver injury in humans. *Genome Res.* **19**:1507-15.

Heinloth AN, Irwin RD, Boorman GA, Nettesheim P, Fannin RD, Sieber SO, Snell ML, Tucker CJ, Li L, Travlos GS, Vansant G, Blackshear PE, Tennant RW, Cunningham ML, and Paules RS (2004) Gene expression profiling of rat livers reveals indicators of potential adverse effects. *Toxicol Sci* **80**:193-202.

Hinson JA, Roberts DW, and James LP (2010) Mechanisms of acetaminophen-induced liver necrosis. *Handb Exp Pharmacol* **196**:369-405.

Ito Y, Abril ER, Bethea NW, McCuskey MK, and McCuskey RS (2006) Dietary steatotic liver attenuates acetaminophen hepatotoxicity in mice. *Microcirculation* **13**:19-27.

Jaeschke H and Bajt ML (2006) Intracellular signaling mechanisms of acetaminophen-induced liver cell death. *Toxicol Sci* **89**:31-41.

Kon K, Ikejima K, Okumura K, Arai K, Aoyama T, and Watanabe S (2010) Diabetic KK-Ay mice are highly susceptible to oxidative hepatocellular damage induced by acetaminophen. *Am J Physiol Gastrointest Liver Physiol* **299**:G329-G337.

Kučera O, Roušar T, Staňková P, Haňáčková L, Lotková H, Podhola M, and Cervinková Z (2012) Susceptibility of rat non-alcoholic fatty liver to the acute toxic effect of acetaminophen. J *Gastroenterol Hepatol* **27**:323-330

Kučera O, Lotková H, Staňková P, Podhola M, Roušar T, Mezera V, and Cervinková Z (2011) Is rat liver affected by non-alcoholic steatosis more susceptible to the acute toxic effect of thioacetamide? *Int J Exp Pathol* **92**:281-289.

Labbe G, Pessayre D, and Fromenty B (2008) Drug-induced liver injury through mitochondrial dysfunction: mechanisms and detection during preclinical safety studies. Fundam *Clin Pharmacol* **22**:335-353.

Landin JS, Cohen SD, and Khairallah EA (1996) Identification of a 54-kDa mitochondrial acetaminophen-binding protein as aldehyde dehydrogenase. *Toxicol Appl Pharmacol* **14**:299-307.

Larson AM, Polson J, Fontana RJ, Davern TJ, Lalani E, Hynan LS, Reisch JS, Schiødt FV, Ostapowicz G, Shakil AO, and Lee WM (2005) Acetaminophen-induced acute liver failure: results of a United States multicenter, prospective study. *Hepatology* **42**:1364-1372.

Lee JK, Abe K, Bridges AS, Patel NJ, Raub TJ, Pollack GM, and Brouwer KL (2009) Sex-dependent disposition of acetaminophen sulfate and glucuronide in the in situ perfused mouse liver. *Drug Metab Dispos* **37**:1916-1921.

Li Z, Yang S, Lin H, Huang J, Watkins PA, Moser AB, Desimone C, Song XY, and Diehl AM (2003) Probiotics and antibodies to TNF inhibit inflammatory activity and improve nonalcoholic fatty liver disease. *Hepatology* **37**:343-350.

Lindström P (2007) The physiology of obese-hyperglycemic mice [ob/ob mice]. *ScientificWorldJournal* 7:666-685.

Liu HH, Lu P, Guo Y, Farrell E, Zhang X, Zheng M, Bosano B, Zhang Z, Allard J, Liao G, Fu S, Chen J, Dolim K, Kuroda A, Usuka J, Cheng J, Tao W, Welch K, Liu Y, Pease J, de Keczer SA, Masjedizadeh M, Hu JS, Weller P, Garrow T, and Peltz G (2010) An integrative genomic analysis identifies Bhmt2 as a diet-dependent genetic factor protecting against acetaminophen-induced liver toxicity. *Genome Res* **20**:28-35.

Massart J, Robin M, Noury F, Fautrel A, Lettéron P, Bado A, Eliat P, and Fromenty B (2012) Pentoxifylline aggravates fatty liver in obese and diabetic ob/ob mice by increasing intestinal glucose absorption and activating hepatic lipogenesis. *Br J Pharmacol* **165**:1361-1374.

Masubuchi Y, Nakayama J, and Watanabe Y (2011) Sex difference in susceptibility to acetaminophen hepatotoxicity is reversed by buthionine sulfoximine. *Toxicology* **287**:54-60.

McGill MR, Yan HM, Ramachandran A, Murray GJ, Rollins DE, and Jaeschke H (2011) HepaRG cells: a human model to study mechanisms of acetaminophen hepatotoxicity. *Hepatology* **53**:974-982.

Muldrew KL, James LP, Coop L, McCullough SS, Hendrickson HP, Hinson JA, and Mayeux PR (2002) Determination of acetaminophen-protein adducts in mouse liver and serum and human serum after hepatotoxic doses of acetaminophen using high-performance liquid chromatography with electrochemical detection. *Drug Metab Dispos* **30**:446-451.

Myers RP and Shaheen AA (2009) Hepatitis C, alcohol abuse, and unintentional overdoses are risk factors for acetaminophen-related hepatotoxicity. *Hepatology* **49**:1399-1400.

Nguyen GC, Sam J, and Thuluvath PJ (2008) Hepatitis C is a predictor of acute liver injury among hospitalizations for acetaminophen overdose in the United States: a nationwide analysis. *Hepatology* **48**:1336-1341.

Prescott LF (1980) Kinetics and metabolism of paracetamol and phenacetin. *Br J Clin Pharmacol* **10**:291S-298S.

Reinartz A, Ehling J, Leue A, Liedtke C, Schneider U, Kopitz J, Weiss T, Hellerbrand C, Weiskirchen R, Knüchel R, and Gassler N (2010) Lipid-induced up-regulation of human acyl-CoA synthetase 5 promotes hepatocellular apoptosis. *Biochim Biophys Acta* **1801**:1025-1035.

Robin MA, Demeilliers C, Sutton A, Paradis V, Maisonneuve C, Dubois S, Poirel O, Lettéron P, Pessayre D, and Fromenty B (2005a) Alcohol increases tumor necrosis factor α and decreases nuclear factor-κB to activate hepatic apoptosis in genetically obese mice. *Hepatology* **42**:1280-1290.

Robin MA, Sauvage I, Grandperret T, Descatoire V, Pessayre D, and Fromenty B (2005b) Ethanol increases mitochondrial cytochrome P450 2E1 in mouse liver and rat hepatocytes. *FEBS Lett* **579**:6895-6902.

Ryan PM, Bourdi M, Korrapati MC, Proctor WR, Vasquez RA, Yee SB, Quinn TD, Chakraborty M, and Pohl LR (2012) Endogenous interleukin-4 regulates glutathione synthesis following acetaminophen-induced liver injury in mice. *Chem Res Toxicol* **25**:83-93.

Sahai A, Malladi P, Pan X, Paul R, Melin-Aldana H, Green RM, and Whitington PF (2004) Obese and diabetic db/db mice develop marked liver fibrosis in a model of nonalcoholic steatohepatitis: role of short-form leptin receptors and osteopontin. *Am J Physiol Gastrointest Liver Physiol* **287**:G1035-G1043.

Sawant SP, Dnyanmote AV, Mitra MS, Chilakapati J, Warbritton A, Latendresse JR, and Mehendale HM (2006) Protective effect of type 2 diabetes on acetaminophen-induced hepatotoxicity in male Swiss-Webster mice. *J Pharmacol Exp Ther* **316**:507-519.

Shinohara M, Ybanez MD, Win S, Than TA, Jain S, Gaarde WA, Han D, and Kaplowitz N (2010) Silencing glycogen synthase kinase-3beta inhibits acetaminophen hepatotoxicity and attenuates JNK activation and loss of glutamate cysteine ligase and myeloid cell leukemia sequence 1. *J Biol Chem* **285**:8244-8255.

Tarantino G, Conca P, Basile V, Gentile A, Capone D, Polichetti G, and Leo E (2007) A prospective study of acute drug-induced liver injury in patients suffering from non-alcoholic fatty liver disease. *Hepatol Res* **37**:410-415.

Tirmenstein MA and Nelson SD (1989) Subcellular binding and effects on calcium homeostasis produced by acetaminophen and a nonhepatotoxic regioisomer, 3'-hydroxyacetanilide, in mouse liver. *J Biol Chem* **264**:9814-9819.

Trak-Smayra V, Paradis V, Massart J, Nasser S, Jebara V, and Fromenty B (2011) Pathology of the liver in obese and diabetic ob/ob and db/db mice fed a standard or high-calorie diet. *Int J Exp Pathol* **92**:413-421.

Tsokos-Kuhn JO, Hughes H, Smith CV, and Mitchell JR (1988) Alkylation of the liver plasma membrane and inhibition of the Ca^{2+} ATPase by acetaminophen. *Biochem Pharmacol* **37**:2125-2131.

Wang Z, Hall SD, Maya JF, Li L, Asghar A, and Gorski JC (2003). Diabetes mellitus increases the in vivo activity of cytochrome P450 2E1 in humans. *Br J Clin Pharmacol* **55**:77-85.

Xu J, Kulkarni SR, Li L, and Slitt A (2012) UDP-glucuronosyltransferase expression in mouse liver is increased in obesity and fasting-induced steatosis. *Drug Metab Dispos* **40**:259-66.

Yohe HC, O'Hara KA, Hunt JA, Kitzmiller TJ, Wood SG, Bement JL, Bement WJ, Szakacs JG, Wrighton SA, Jacobs JM, Kostrubsky V, Sinclair PR, and Sinclair JF (2006) Involvement of Toll-like receptor 4 in acetaminophen hepatotoxicity. *Am J Physiol Gastrointest Liver Physiol* **290**:G1269-G1279.

Zhao P and Slattery JT (2002) Effects of ethanol dose and ethanol withdrawal on rat liver mitochondrial glutathione: implication of potentiated acetaminophen toxicity in alcoholics. *Drug Metab Dispos* **30**:1413-141.

JPET Fast Forward. Published on May 30, 2012 as DOI: 10.1124/jpet.112.193813
This article has not been copyedited and formatted. The final version may differ from this version.

Footnotes

This work was supported by INSERM (Institut Nationale de la Santé et de la Recherche Médicale). Jacinthe Aubert and Karima Begriche were recipients of grants from the President of Rennes 1 University, and the Région Bretagne, respectively.

The authors declare no conflict of interest

JPET Fast Forward. Published on May 30, 2012 as DOI: 10.1124/jpet.112.193813
This article has not been copyedited and formatted. The final version may differ from this version.

Figure Legends

Figure 1: Hepatic steatosis and liver lipids in untreated female ob/ob and db/db mice. (A) Hepatic histology assessed with the HES staining. (a and b) Representative pictures of an ob/ob mouse liver with a combination of macrovacuolar and microvesicular steatosis at 100x and 200x magnification, respectively. (c and d) Representative pictures of a db/db mouse liver with microvesicular steatosis at 100x and 200x magnification, respectively. The scale on each picture corresponds to 100 μm. The symbol * in the different pictures indicates a central vein. (B) Liver lipids and triglycerides in female ob/ob and db/db mice. Results are means ± SEM for 8 mice per group. *Significantly different from db/db mice (P<0.05).

Figure 2: Plasma transaminases and liver histology before and 8 h after APAP intoxication in female wild-type, ob/ob and db/db mice. (A) Basal plasma transaminases in all untreated female wild-type, ob/ob and db/db mice used in the present study. Results are means ± SEM for 24-30 mice per group. *Different from lean mice (P<0.05). (B) Plasma transaminases 8 h after APAP intoxication. Results are means ± SEM for 9 mice per group. *Significantly different from lean and ob/ob mice (P<0.05). (C) Hepatic histology before (a, d, g) and 8 h after APAP intoxication (b, c, e, f, h, i). After APAP intoxication, areas of necrosis are delimited by dotted lines. (a, b, c) Representative pictures of wild-type mouse livers at 100x (a, b) and 200x (c) magnification. Yellow arrows in picture c indicate vacuoles of lipids. (d, e, f) Representative pictures of ob/ob mouse livers at 100x (d, e) and 200x (c) magnification. (g, h, i) Representative pictures of db/db mouse livers at 100x (g, h) and 200x (c) magnification. The scale on each picture corresponds to 200 μm. The symbol * in the different pictures indicates a central vein.

Figure 3: Hepatic TUNEL assay before and 8 h after APAP intoxication in female wild-type, ob/ob and db/db mice. (A) TUNEL assay before (a, d, g) and 8 h after APAP intoxication (b, c, e, f, h, i) in wild-type mice (a, b, c), ob/ob mice (d, e, f) and db/db mice (g, h, i). Pictures a, b, d, e, g and h are at 100x magnification, whereas pictures c, f and i are magnification (200x) of the boxed areas shown in the upper pictures. The scale on each picture corresponds to 200 μm. The symbol * in the different pictures indicates a central vein. (B) Percentage of TUNEL-positive nuclei 8 h after APAP intoxication in wild-type, ob/ob and db/db mice (n = 6-9 mice per group). Data are represented as median with interquartile range (25^{th}-75^{th} percentiles). *Significantly different from ob/ob mice (P<0.05).

JPET Fast Forward. Published on May 30, 2012 as DOI: 10.1124/jpet.112.193813
This article has not been copyedited and formatted. The final version may differ from this version.

Figure 4: Hepatic levels of GSH and APAP-protein adducts in female wild-type, ob/ob and db/db mice. (A) Hepatic GSH levels before and 0.5, 2, 4 and 8 h after APAP intoxication. After APAP treatment, results are means ± SEM for 7-12 mice per group. For GSH levels before treatment (controls), values from the different time points were pooled and thus, results are means ± SEM for 20-22 mice per group. The letters G and T above the bars indicate a significant effect ($P<0.05$) of the genotype and treatment, respectively. *Different from ob/ob and db/db mice ($P<0.05$). For clarity, the significant effect of APAP treatment at the different time points is not indicated by another symbol. (B) Hepatic levels of APAP-protein adducts 0.5, 2, 4 and 8 h after APAP intoxication. Results are means ± SEM for 6-8 mice per group. The letter G above the bars indicates a significant effect ($P<0.05$) of the genotype. *Significantly different from ob/ob and db/db mice ($P<0.05$). APAP-protein adducts in untreated mice were undetectable (data not shown).

Figure 5: Liver protein expression of total and phosphorylated JNK in female wild-type (wt), ob/ob and db/db mice 2, 4 and 8 h after APAP intoxication. In the western blots representative of 3 different mice per genotype, the upper and lower bands of JNK and phosphorylated JNK (P-JNK) represent the p54 and p46 isoforms of JNK, respectively. Levels of JNK and P-JNK (means ± SEM) were assessed in 6 different mice per genotype, and respective values were normalized with HSC70. *Significantly different from the other genotypes ($P<0.05$).

Figure 6: Hepatic mRNA expression of genes in female wild-type (wt), ob/ob (ob) and db/db (db) mice 0.5, 2, 4 and 8 h after APAP intoxication (Panels A, B, C and D, respectively). mRNA expression of 12 different genes was determined by RT-qPCR. Results are means ± SEM for 7-9 mice per group. Dark and light bars represent control and treated mice, respectively. In the upper-right corner of each box, letters G, T and GxT indicate a significant effect ($P<0.05$) of genotype, an effect of treatment, and an interaction between genotype and treatment, respectively. Significantly different ($P<0.05$) from *other genotypes, $^{\#}$wild-type mice, †db/db mice. For clarity, the significant effect of APAP treatment in some groups of animals is not indicated by another symbol.

JPET Fast Forward. Published on May 30, 2012 as DOI: 10.1124/jpet.112.193813
This article has not been copyedited and formatted. The final version may differ from this version.

Table 1. Body parameters, plasma glucose, and hepatic CYP2E1 activity in male and female wild-type, ob/ob and db/db mice

Groups of mice	Body parameters and plasma glucose				Hepatic CYP2E1 activity	
	Body weight (g)	Liver weight (g)	Liver to body weight ratio (%)	Plasma glucose (mM)	Aniline hydroxylase	Chlorzoxazone hydroxylase
wild-type male	22.1 ± 0.8	0.97 ± 0.06	4.4 ± 0.1	7.1 ± 0.1	0.79 ± 0.03	1.96 ± 0.14
wild-type female	17.2 ± 0.4	0.77 ± 0.04	4.5 ± 0.2	7.1 ± 0.5	0.89 ± 0.02	1.96 ± 0.13
ob/ob male	44.2 ± 0.4	2.98 ± 0.13	6.7 ± 0.3	12.4 ± 1.2	0.85 ± 0.07	1.84 ± 0.26
ob/ob female	43.4 ± 0.4	2.97 ± 0.09	6.8± 0.1	17.9 ± 1.1	0.93 ± 0.05	1.88 ± 0.27
db/db male	40.2 ± 1.7	1.97 ± 0.18	4.9± 0.3	20.1 ± 2.9	1.18 ± 0.05*	1.82 ± 0.20
db/db female	39.6 ± 0.6	1.89 ± 0.04	4.8 ± 0.1	18.6 ± 1.2	1.34 ± 0.08*	3.29 ± 0.78¶
Statistical analysis (2- wayANOVA)	G, S, GxS	G	G	G, GxS	G, S	G, S, GxS

Results are means ± SEM for 6 mice per group. CYP2E1 enzymatic activities are expressed in nmoles.min^{-1}.mg proteins^{-1}. For statistical analysis, the letters G, S and GxS indicate a significant effect (P<0.05) of genotype, an effect of sex, and an interaction between genotype and sex, respectively. For clarity, significant differences with the Tukey's HSD test are given only for CYP2E1 activities: *significantly different (P<0.05) from the other genotypes, ¶significantly different (P<0.05) from the other groups.

JPET Fast Forward. Published on May 30, 2012 as DOI: 10.1124/jpet.112.193813
This article has not been copyedited and formatted. The final version may differ from this version.

Table 2. Hepatic mtDNA levels and plasma lactate and β-hydroxybutyrate in female wild-type, ob/ob and db/db mice

Time	Group of mice	Hepatic mtDNA levels (AU)	Plasma lactate concentration (mM)	Plasma β-hydroxybutyrate concentration (mM)
2 h	wild-type	1.00 ± 0.21	2.2 ± 0.4	0.62 ± 0.03
	wild-type + APAP	1.39 ± 0.14	1.7 ± 0.1	0.11 ± 0.01
	ob/ob	1.71 ± 0.21	2.9 ± 0.3	0.75 ± 0.15
	ob/ob + APAP	1.17 ± 0.03	1.6 ± 0.4	1.85 ± 0.48
	db/db	1.30 ± 0.18	3.2 ± 0.2	0.73 ± 0.15
	db/db + APAP	1.19 ± 0.28	1.9 ± 0.3	1.20 ± 0.37
	Statistical analysis (2-way ANOVA)	GxT	T	G, GxT
4 h	wild-type	0.95 ± 0.20	2.7 ± 0.4	0.85 ± 0.21
	wild-type + APAP	1.24 ± 0.22	1.9 ± 0.3	0.40 ± 0.05
	ob/ob	1.62 ± 0.20	2.2 ± 0.3	1.20 ± 0.26
	ob/ob + APAP	1.60 ± 0.67	0.7 ± 0.1	0.16 ± 0.15
	db/db	1.22 ± 0.17	3.1 ± 0.5	1.05 ± 0.23
	db/db + APAP	1.43 ± 0.24	2.3 ± 0.2	0.22 ± 0.03
	Statistical analysis (2-way ANOVA)		G, T	G, T, GxT
8 h	wild-type	1.12 ± 0.21	2.7 ± 0.2	0.98 ± 0.06
	wild-type + APAP	2.70 ± 0.56	1.3 ± 0.2	5.02 ± 0.82
	ob/ob	1.91 ± 0.19	2.7 ± 0.5	1.55 ± 0.23
	ob/ob + APAP	2.71 ± 0.27	0.9 ± 0.1	6.21 ± 1.76
	db/db	1.45 ± 0.18	2.8 ± 0.3	2.21 ± 0.51
	db/db + APAP	2.80 ± 0.36	2.2 ± 0.1	1.78 ± 0.34
	Statistical analysis (2-way ANOVA)	T	G, T	T

Results are means ± SEM for 4-5 mice per group for hepatic mtDNA levels and 4-6 mice per group for plasma lactate and β-hydroxybutyrate. For statistical analysis, the letters G, T and GxT indicate a significant effect (P<0.05) of genotype, an effect of treatment, and an interaction between genotype and treatment, respectively. For clarity, significant differences with the Tukey's HSD test are not given in this Table.

JPET Fast Forward. Published on May 30, 2012 as DOI: 10.1124/jpet.112.193813
This article has not been copyedited and formatted. The final version may differ from this version.

Table 3. Plasma levels of APAP, APAP-sulfate and APAP-glucuronide in female wild-type, ob/ob and db/db mice

Time	Group of mice	APAP (mg/L)	APAP-sulfate (mg/L)	APAP-glucuronide (mg/L)
0.5 h	wild-type + APAP	364 ± 13*	66 ± 3	425 ± 38*
	ob/ob + APAP	599 ± 56	80 ± 9	2055 ± 253*
	db/db + APAP	541 ± 31	64 ± 6	1294 ± 206*
	Statistical analysis (one-way ANOVA)	G	-	G
2 h	wild-type + APAP	188 ± 15*	57 ± 2*	370 ± 44*
	ob/ob + APAP	289 ± 30	106 ± 7	1860 ± 220
	db/db + APAP	297 ±46	87 ± 6	1322 ± 190
	Statistical analysis (one-way ANOVA)	G	G	G
4 h	wild-type + APAP	158 ± 36*	63 ± 15	46 ± 17
	ob/ob + APAP	22 ± 8	41 ± 18	159 ± 109
	db/db + APAP	43 ± 23	14 ± 3	63 ± 33
	Statistical analysis (one-way ANOVA)	G	-	-
8 h	wild-type + APAP	12 ±7	21 ± 6	11 ± 9
	ob/ob + APAP	2 ± 1	23 ± 11	197 ± 128
	db/db + APAP	3 ± 1	15 ± 7	48 ± 19
	Statistical analysis (one-way ANOVA)	-	-	-

Results are means ± SEM for 6-9 mice per group. For statistical analysis, the letter G indicates a significant effect (P<0.05) of genotype. *Different from other genotypes (P<0.05), as assessed by the Tukey's HSD test.

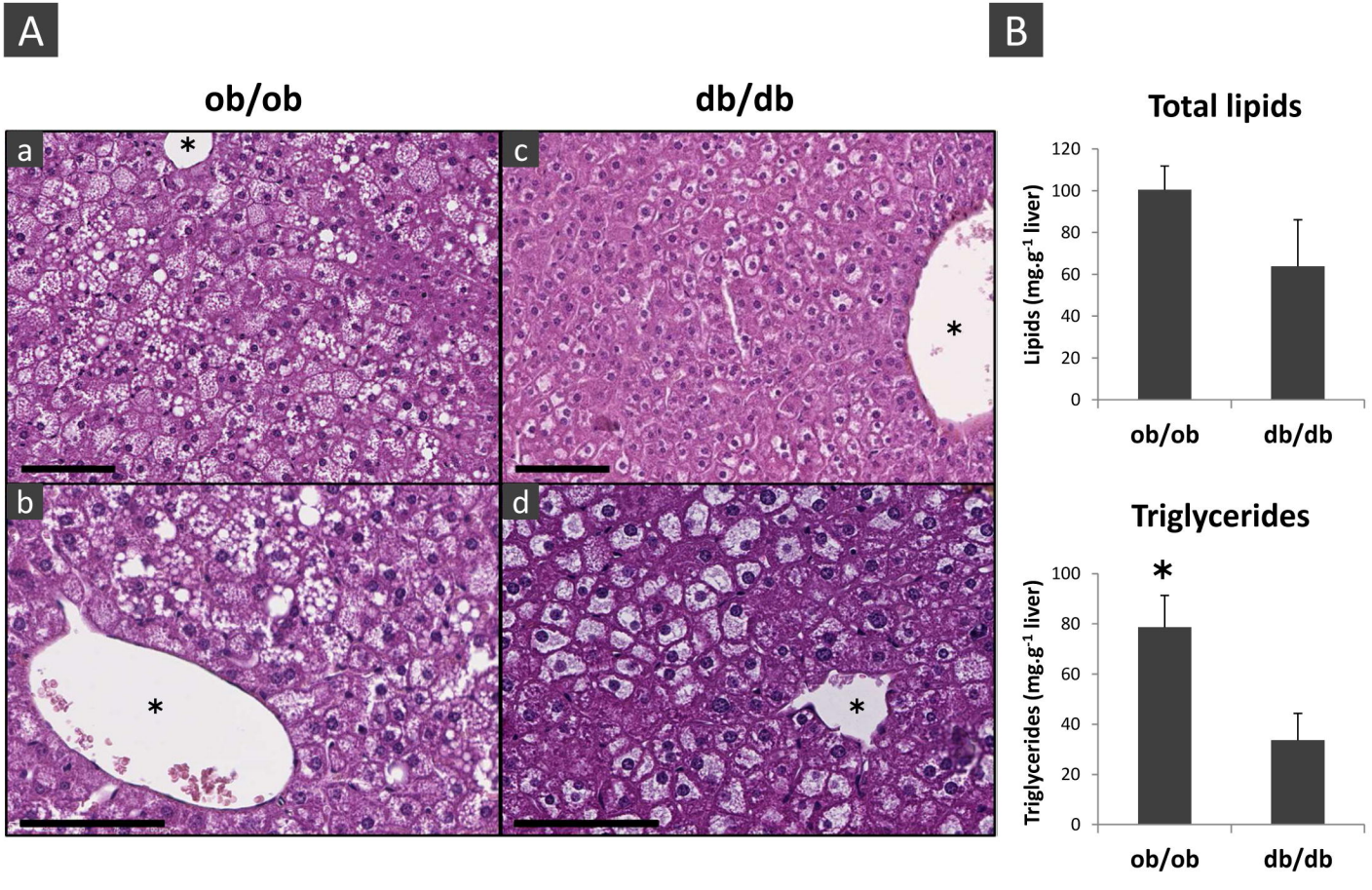
A
ob/ob
db/db
a
b
c
d
B
Total lipids
Lipids (mg.g-1 liver)
120
100
80
60
40
20
0
ob/ob
db/db
Triglycerides
Triglycerides (mg.g-1 liver)
100
80
60
40
20
0
ob/ob
db/db

Figure 1

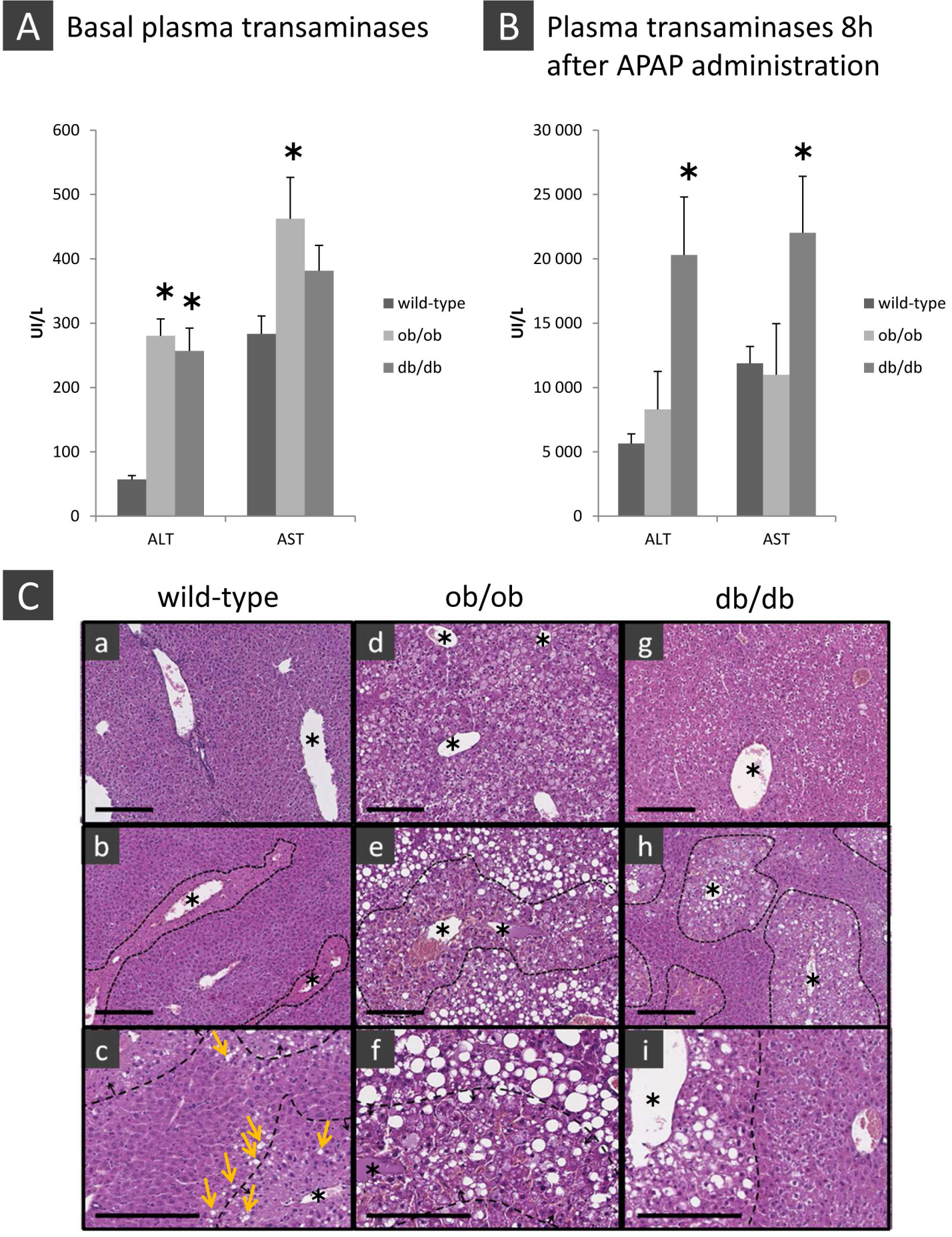
A
Basal plasma transaminases
B
Plasma transaminases 8h after APAP administration
UI/L
600
500
400
300
200
100
0
ALT
AST
wild-type
ob/ob
db/db
30 000
25 000
20 000
15 000
10 000
5 000
C
wild-type
ob/ob
db/db
a
b
c
d
e
f
g
h
i

Figure 2

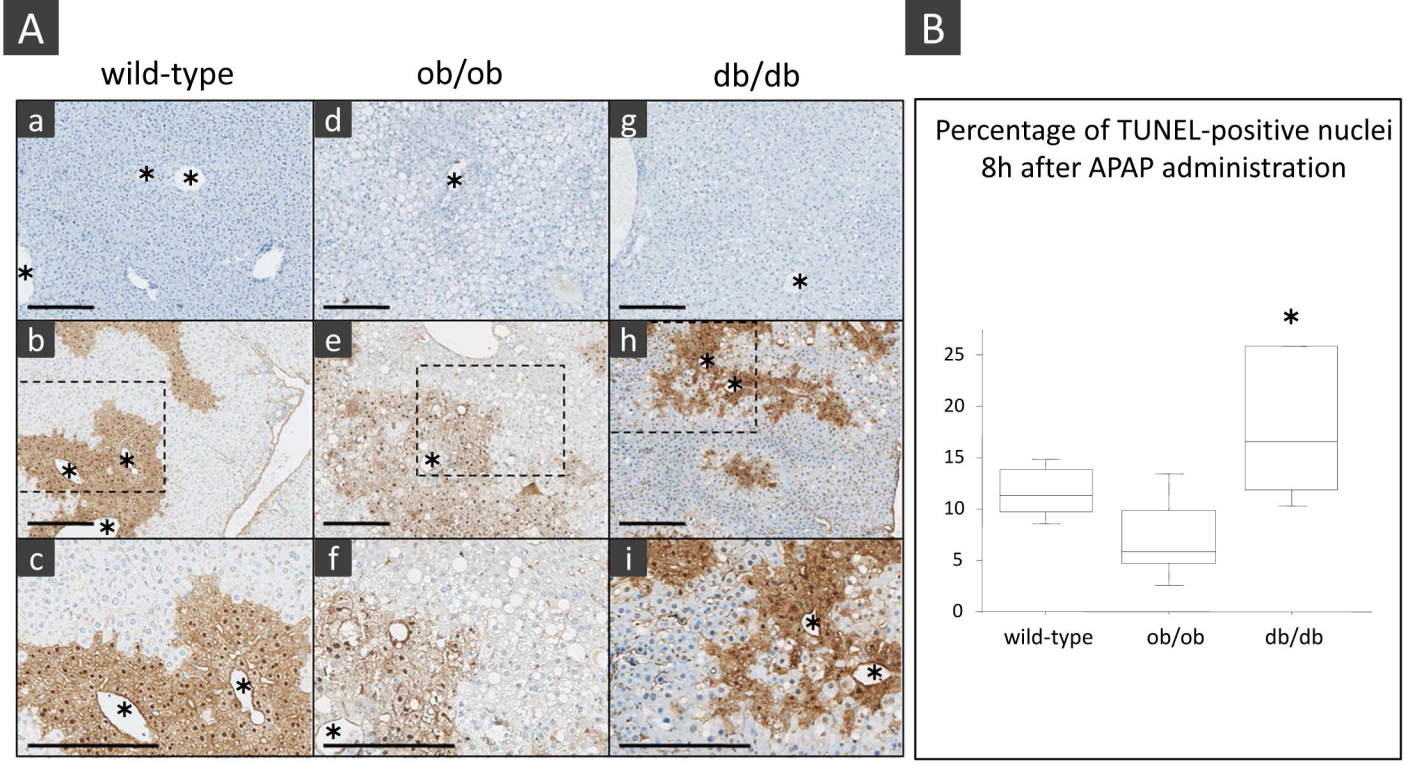
A
wild-type
ob/ob
db/db
a
b
c
d
e
f
g
h
i
B
Percentage of TUNEL-positive nuclei
8h after APAP administration
25
20
15
10
5
0
wild-type
ob/ob
db/db

Figure 3

A Hepatic GSH levels

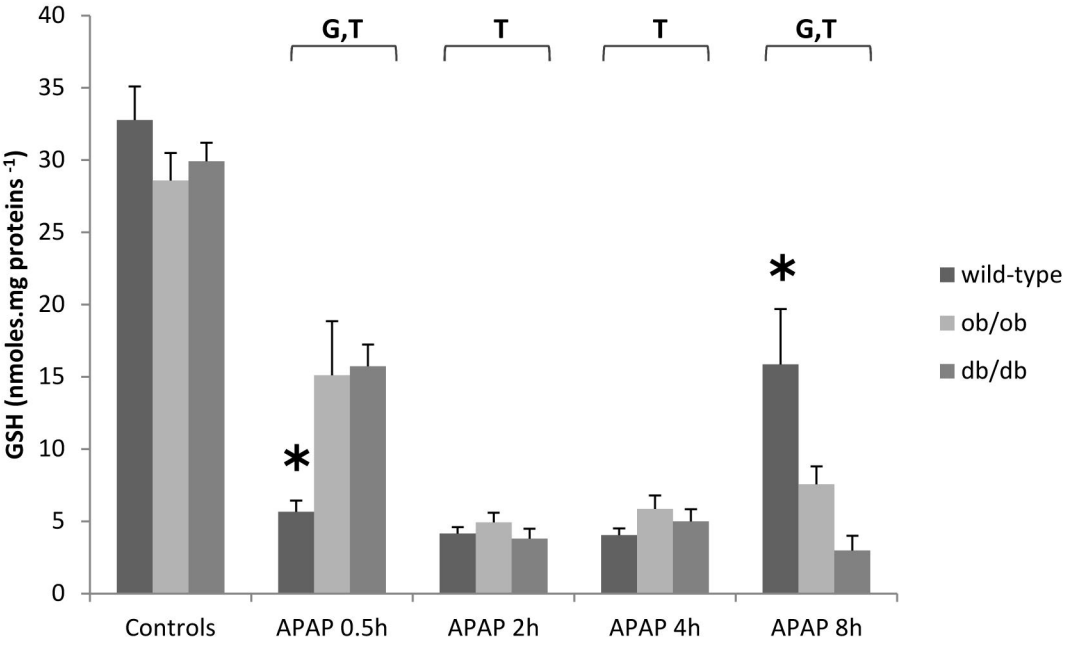

B Hepatic levels of APAP-protein adducts

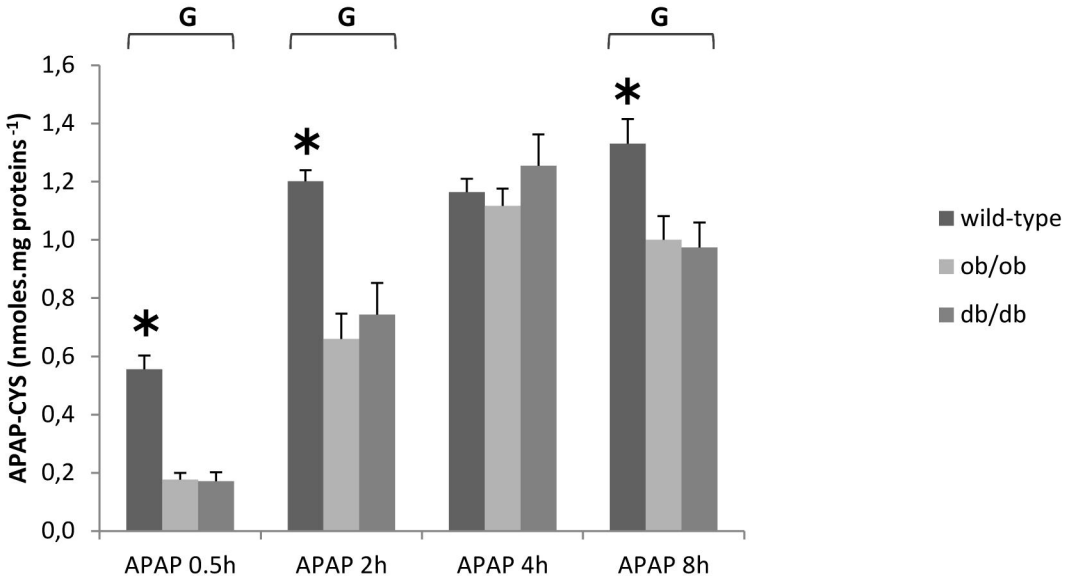

Figure 4

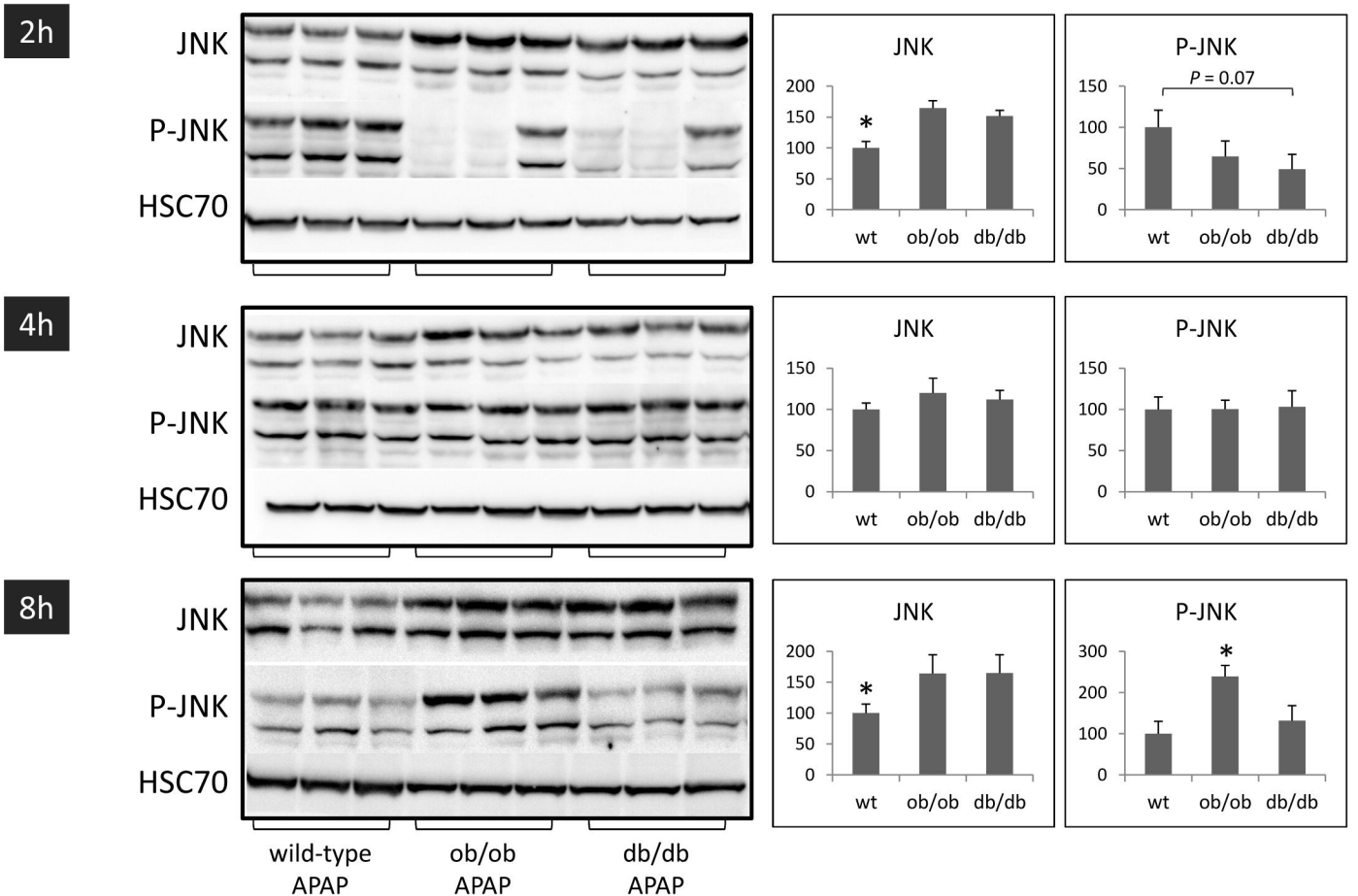
2h
4h
8h
JNK
P-JNK
HSC70
wild-type APAP
ob/ob APAP
db/db APAP
JNK
P-JNK
P = 0.07
wt
ob/ob
db/db
*

Figure 5

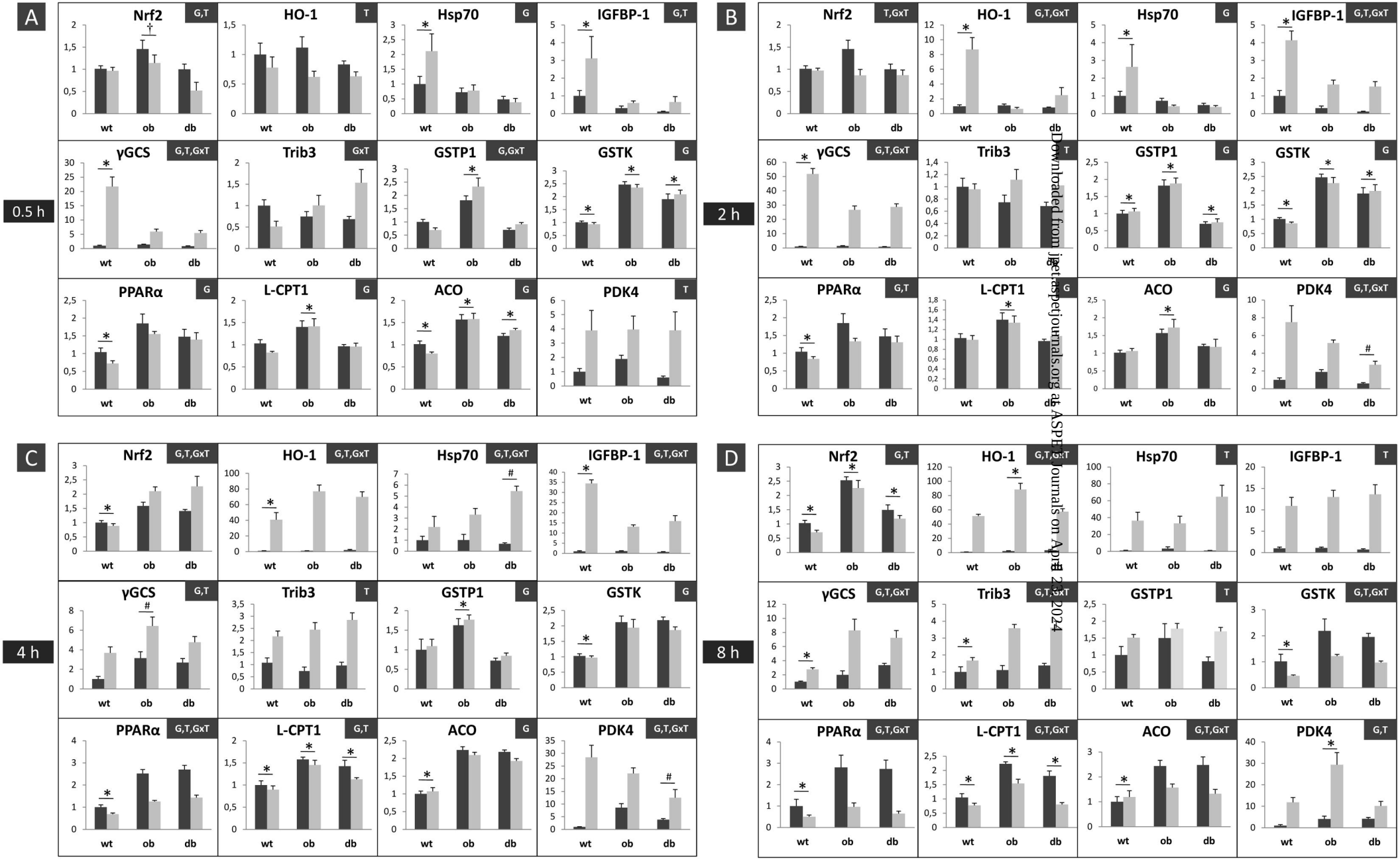

Figure 6